RESEARCH ARTICLE

Reliability Assessment and Optimization of Multi-State Aggregated Grid Systems Based on V2G Technology

Xu Yang[1], **Peng Su**[1,2,*] and **Yuzhe Dong**[3]

[1] School of Economics and Management, North University of China, Taiyuan 030051, China
[2] Shanxi Transportation Technology Research & Development Co., LTD, Taiyuan 030032, China
[3] School of Vehicle and Transportation Engineering, Taiyuan University of Science and Technology of China, Taiyuan 030024, China

Abstract

In recent years, while the rapid development of global electric vehicles (EVs) has been driving energy transition, their large-scale integration into power grids has posed significant challenges to the stability of power systems and the reliability of electricity supply. Vehicle-to-Grid (V2G) technology demonstrates potential in balancing grid peak-valley differences and facilitating renewable energy integration, thereby effectively mitigating issues caused by disorderly grid integration of massive EVs. This paper proposes a "Vehicle-to-Station-to-Grid" (VSG) aggregated system based on V2G technology. In this system, the multi-state stochastic power output and demand of EVs are considered. Power generated by an EV is allocated to other EVs in need through power transmission lines with transmission losses and capacity constraints. This achieves dynamic power distribution within the "Vehicle-to-Station" Subsystem (VSS). A reliability evaluation model for the VSS is established using the universal generating function (UGF) method. An electric vehicle aggregator (EVA) is introduced as an energy storage container to enable bidirectional power interaction between the VSS and the grid subsystem. This further establishes the reliability model of the VSG aggregation system. This paper specifically analyzes two scenarios: with and without transmission losses. The effectiveness of the reliability models for the VSS and the VSG aggregation system is verified through theoretical derivation and numerical examples. Sensitivity analysis is conducted to clarify the impact of transmission losses on reliability. Finally, a goal programming model is established under constraints, and an optimization strategy for EVs based on a power-sharing mechanism is proposed within the VSG aggregation system.

Keywords: vehicle-to-grid, multi-state systems, power sharing, reliability.

1 Introduction

In recent years, there have been different research advancements on performance sharing both domestically and internationally. For example, Levitin extended the performance sharing model for multi-state components [1]. In this model, excess

Submitted: 14 April 2026
Accepted: 06 May 2026
Published: 11 May 2026

Vol. 2, **No.** 2, 2026.
10.62762/TSSR.2026.977328

***Corresponding author:**
Peng Su
supeng@nuc.edu.cn

Citation
Yang, X., Su, P., & Dong, Y. (2026). Reliability Assessment and Optimization of Multi-State Aggregated Grid Systems Based on V2G Technology. *ICCK Transactions on Systems Safety and Reliability*, 2(2), 123–139.

performance can be transferred, but the transferred performance is limited by the stochastic capacity of the transmission system. The reliability and performance deficiency were evaluated using the universal generating function (UGF) method.

Subsequently, many scholars have carried out further optimization and extension studies based on this system model. Zhao et al. [2] extended the common bus performance sharing model to the k-out-of-n: G structure, analyzing reliability of multi-state systems in which each component shares surplus performance with others through a common bus under transmission capacity constraints. Wang et al. [3] proposed a new reliability model for a multi-state system (MSS) with N series-connected units. Excess performance can only be transmitted to adjacent units through a limited-capacity intermediate transmitter. If the demand of any unit is not satisfied, the system will fail. Qiu and Ming [4] were among the first to incorporate transmission loss into common bus performance sharing systems, defining transmission loss as a function of transmission distance and the performance transmitted, and evaluating reliability via the UGF method. Based on the conventional performance sharing model, Peng [5] studied a multi-state system with hierarchical performance sharing groups. The system consists of multiple subsystems connected by a main bus, while internal component groups share performance through auxiliary buses. The system reliability was evaluated using the UGF method, and the optimal allocation of components was investigated. Su et al. [6] proposed a multi-state complex series system based on k-out-of-n: G subsystems for multi-state phased-mission systems with performance sharing via a common bus. They considered component failures and subsystem faults, and accounted for transmission capacity constraints during performance sharing. The system reliability was calculated using a bivariate UGF algorithm. Jia et al. [7] proposed a reliability model for power systems integrating multi-state warm standby with a performance sharing mechanism, evaluating system reliability using a multi-state decision diagram technique combined with the UGF method. Bhatt et al. [8] constructed a weighted reliability model considering multi-stage missions and dynamic performance allocation. They evaluated system availability using Markov processes and UGF method. An optimal allocation algorithm was developed to achieve efficient performance sharing. The effectiveness of the model was demonstrated using a hybrid wind-solar distribution system as an example.

To enhance the reliability of various system models, some scholars have conducted optimization studies based on analyzing the key factors affecting system reliability, aiming to achieve optimal performance metrics. Xiao et al. [9] proposed a multi-state system with two-level performance sharing. In this system, unique performance transmitters are installed between any adjacent subsystems or components, allowing only the excess performance to be transferred to neighboring units. Since component allocation and sequencing significantly impact system reliability, a genetic algorithm was employed to obtain the optimal allocation and sequencing of components. Cheng et al. [10] studied a multi-state phased mission system with k-out-of-n(G) subsystems and common bus performance sharing, considering common cause failures and evaluating system reliability using the UGF method. Su et al. [11] investigated a k-out-of-(n+1):G multi-state system (MSS) with a performance sharing mechanism and calculated its reliability under a star topology configuration.

After completing detailed theoretical derivations, many scholars have integrated reliability models with practical engineering applications, taking into account factors of performance loss. Yi et al. [12] fully considered that performance loss occurs to some extent during the sharing of capacity due to various influencing factors. They took into account that power transmission loss is affected by three factors: temperature, distance, and humidity. Based on this, they proposed three different models with transmission loss. Azhdari and Ardakan [13] studied a multi-state star network with a two-layer performance sharing mechanism.

Considering that actual performance sharing involves transmission losses, they addressed the issue of transmission loss from two aspects. During the reliability assessment process, some scholars have introduced new evaluation methods. Wu et al. [14] proposed a reliability model for multi-state performance sharing systems subject to transmission loss and random shocks, incorporating Markov processes and the UGF technique to evaluate system reliability under a dynamic operating environment. Wu et al. [15] proposed a reliability model for a weighted k-out-of-n:G performance sharing system considering stochastic shocks and transmission losses. The model accounts for losses and enables dynamic performance allocation among components via a common bus. Gu et al. [16] introduced a strategy space reduction to improve the genetic algorithm for optimizing transmission capacity allocation in tree-structured performance sharing systems. With the widespread adoption of electric vehicles (EVs), many scholars have investigated the interaction between the power grid and EVs. Liu et al. [17] developed an agent-based model integrating EVs and V2G technology, which provides a basis for relevant policy-making and technology investment. Ma et al. [18] developed a new power system planning model to jointly optimize investment and operational decisions in the power system. They analyzed both one-way and two-way V2G modes.

From a technical perspective, Peng [19] analyzed the V2G energy allocation and output capacity of a single charging station which used network theory and a hybrid evolutionary algorithm. The study also optimized a complex service network formed by multiple V2G charging stations and energy customers. Lee et al. [20] used a method combining discrete choice experiments with energy storage expansion planning. They found that under nighttime conditions and appropriate incentive compensation, V2G can significantly reduce the energy storage capacity requirements, peak net load, and total costs in a power system dominated by renewable energy. Some scholars have deeply analyzed V2G technology from the angles of social and technical feasibility. Sagaria et al. [21] developed a simulation model using Germany as an example to analyze the impact of technical factors on V2G technology. The results show that V2G technology can effectively improve the reliability of the power grid.

In the field of research on the acceptance behavior of V2G technology, relevant scholars have conducted in-depth explorations. Liu et al. [22] comprehensively analyzed the acceptance behavior of vehicle-to-grid (V2G) technology and proposed potential directions for future research. Su et al. [23] developed a multi-state aggregation grid reliability assessment model based on continuous-time Markov processes and UGF method, and quantitatively analyzed the impact of large-scale integration of EVs on the operational stability of the power grid. The core contribution lies in the development of a dynamic reliability assessment framework. This framework combines continuous-time Markov processes with UGF to describe the random degradation process of system components over continuous time. In specific application scenarios, some scholars have provided concrete cases and data support for the application of V2G technology in practical situations. Comi and Elnour [24] explored the potential of setting up V2G hubs in high-demand areas to optimize energy transfer and enhance grid stability and efficiency. Du et al. [25] built an integrated model of transportation networks and urban delivery systems based on real data from Shanghai. They analyzed the potential of EVs to serve as auxiliary power sources after disasters. Some scholars have focused on the impact of V2G technology on the battery life of EVs and conducted in-depth research. Kouzelis et al. [26] used high-precision battery simulation models and semi-empirical aging models to quantify capacity degradation. This allowed them to accurately assess the impact of V2G technology on the battery life of EVs. In terms of optimization strategies, Li et al. [27] proposed a V2G multi-objective scheduling strategy based on user behavior. By combining load curves and electricity pricing mechanisms, they optimized the charging and discharging of EV fleets to maximize the benefits of power response. Prencipe et al. [28] proposed a mixed-integer linear programming model to optimize vehicle allocation and charging-discharging scheduling. Shaheen et al. [29] proposed a V2G scheduling method based on metaheuristic algorithms to optimize the charging and discharging strategies of EVs during their parking periods. Liu et al. [30] proposed an Adaptive V2G Re-allocation method. By constructing a transition model and using an adaptive boosting algorithm, it maximizes V2G transmission capacity while ensuring punctuality. These studies provide effective methods for the optimal scheduling of V2G technology. Zhang et al. [31] developed a V2G queue aggregation model. It optimizes charging and discharging schedules while ensuring real-time charging demands. One important direction of current research is to combine V2G technology with performance sharing mechanisms. In terms of performance sharing, V2G technology offers new possibilities for energy interaction between EVs and the power grid.

This paper focuses on the reliability evaluation of a multi-state aggregated power grid system in a V2G environment. The multi-state characteristics of EVs and transmission lines are considered. Under the constraints of capacity and transmission loss, a system analysis model that is closer to engineering practice is established. The study is carried out through theoretical derivation, case analysis, and optimization strategy design. The main contributions are as follows: (1) This paper proposes a novel VSG multi-state aggregated power grid system based on a three-layer aggregation architecture. The Electric vehicle aggregator (EVA) is used as an intermediate energy storage node. It integrates the multi-state power supply and demand of EVs and incorporates dynamic transmission capacity and loss constraints. (2) The application scope of the UGF method is extended. By combining discrete probability distribution and dynamic capacity constraints, the analytical reliability expressions of the VSS and VSG aggregation system are derived. This provides an evaluation method for power sharing between EVs and the power grid in the V2G scenario. (3) A dynamic power allocation optimization strategy is designed. A weighted deviation minimization objective function is constructed. The "low energy consumption priority" allocation principle is adopted. This achieves efficient power utilization and coordinated improvement of system reliability, and provides theoretical support for practical system dispatch.

The rest of this paper is organized as follows: Section 2 describes the system operation mechanism and symbol definition. Section 3 analyzes the reliability of the studied system model. Section 4 validates the effectiveness of the methods with specific examples. Section 5 presents relevant optimization techniques. Section 6 concludes the paper.

2 Model Description and Symbol Definition

The detailed description of the main symbols used in this paper is shown in Table 1.

A multi-state aggregated power grid system model based on V2G technology is constructed. The specific structure is shown in Figure 1. The system consists of m VSSs. Each VSS includes n_i EVs with discharging capability and m_i EVs with charging demand. All EVs are connected to the system through charging piles. A three-party verification mechanism is applied to validate and manage charging and discharging permissions and interactions. The charging piles of each VSS are connected to the energy storage battery of the EVA through the first-level power line. The aggregator centrally performs power aggregation, management, and optimal allocation. At the same time, distributed power sources such as thermal power generation and wind power generation can also be connected to this network. Together, they form a VSG aggregation system with coordinated control capability.

Table 1. Description of main symbols.

Symbol	Symbol Description
$G_{i,k}$	The power output of the $k-th$ EV in the $i-th$ VSS.
$W_{i,k}$	The power demand of the $k-th$ EV in the $i-th$ VSS.
G_i	The power output of the $i-th$ VSS.
W_i	The power demand of the $i-th$ VSS.
C_i^1	The capacity of the first-level power transmission line in the $i-th$ VSS.
C_i^2	The capacity of the second-level power transmission line in the $i-th$ VSS.
s	accumulated power
d	missing power
R_i	The reliability of the $i-th$ VSS.
R_s	The reliability of the VSG aggregation system.
θ_0	The initial transmission loss rate
k_1	The decay coefficient of the first-level transmission line loss rate, reflecting the effects of aging and environmental factors $(k_1 \geq 0)$.
k_2	The decay coefficient of the second-level transmission line loss rate $(k_2 \geq 0)$.
θ_1^i	The first-level power transmission lines
θ_2^i	The second-level power transmission lines
S_f	The accumulated power of the VSG aggregation system
D_f	The missing power of the VSG aggregation system
U_{eff}	The effective power
G_{total}	The total effective power output

Taking the $i-th$ VSS as the analysis object, the total power output G_i of EVs with discharging capability and the total power demand W_i of EVs with charging demand are first aggregated. The power is then transmitted to the aggregator through the first-level power line C_i^1. This process must satisfy the line capacity constraint. Under the ideal condition without transmission loss, the transmissible surplus power is $s_{i,v} = \min\{s_{i,v}, c_i^1\}$, and the missing power is $d_{i,v} = \min\{d_{i,v}, c_i^1\}$.

When the first-level transmission loss θ_i^1 is considered, the total power output decreases after transmission, and the total power demand increases due to the loss. Therefore, the transmissible surplus power is revised as $s_{i,v} = \min\{s_{i,v}(1-\theta_i^1), c_i^1\}$, and the missing power

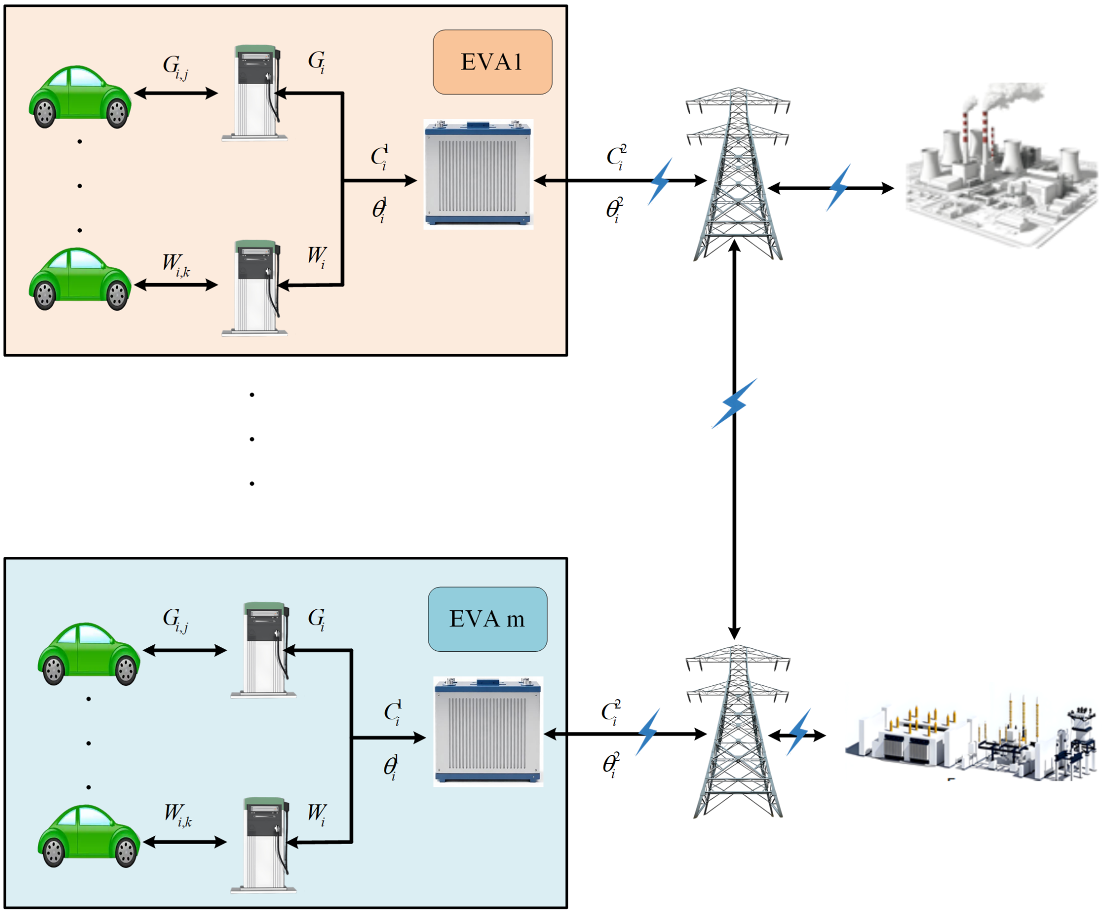

Figure 1. System model structure diagram.

is revised as $d_{i,v} = \min\{d_{i,v}(1+\theta_i^1), c_i^1\}$. Based on this process, the reliability R_i of a single VSS can be calculated.

After completing power sharing within the VSS, the surplus power $s_{i,j}$ or the missing power $d_{i,j}$ is further transmitted through the second-level power line C_i^2. Similarly, under the condition without transmission loss, the transmitted surplus power is $s_{i,k} = \min\{s_{i,j}, c_i^2\}$, and the missing power is $d_{i,k} = \min\{d_{i,j}, (1+\theta_i^2), c_i^2\}$. When transmission loss is considered, the second-level transmission loss θ_i^2 must be included. Accordingly, the surplus power after transmission is revised as $s_{i,k} = \min\{s_{i,j}(1-\theta_i^2), c_i^2\}$, and the missing power is revised as $d_{i,k} = \min\{d_{i,j}(1+\theta_i^2), c_i^2\}$.

Finally, at the VSG aggregation system level, the m VSSs are aggregated and scheduled in an integrated manner. This process achieves complementary matching between surplus power and missing power among subsystems, thereby improving the overall reliability of the VSG aggregation system. The specific operation mechanism and parameter settings of the VSG aggregation system will be described and analyzed in detail in Section 3 of this paper.

3 Reliability analysis based on the UGF method

The multi-state aggregation system proposed in this paper based on V2G technology uses the UGF method to describe the random power output and random power demand states of each EV in the VSS system. Specifically, each EV can be regarded as a multi-state discrete random variable, with random power output levels and power demand levels, which are described using a discrete probability distribution model. In the $i-th$ VSS, the power output $G_{i,k}$ of the $k-th$ EV takes values from the set $\{g_{i,k}^1, g_{i,k}^2, \cdots, g_{i,k}^{h_i^k}\}$. The Probability Mass Function (PMF) of $G_{i,k}$ can be represented using the UGF as follows:

$$U_{G_{i,k}}(z) = \sum_{h=1}^{h_i^k} \alpha_{i,k}^h z^{g_{i,k}^h} \tag{1}$$

Similarly, in the $i-th$ VSS, the power demand $W_{i,k}$ of the $j-th$ EV takes values from the set $\{w_{i,j}^1, w_{i,j}^2, \cdots, w_{i,j}^{l_j^i}\}$. The PMF of $W_{i,k}$ can be represented using the UGF as follows:

$$U_{W_{i,j}}(z) = \sum_{l=1}^{l_j^i} \beta_{i,j}^{l} z^{w_{i,j}^{l}} \tag{2}$$

Based on the above equations, in the $i-th$ VSS, there are n_i EVSs with power output capabilities and m_i EVSs with power demand. Their power output and power demand can be represented by the following random vectors $G_i = \{G_{i1}, G_{i2}, \cdots, G_{in_i}\}$ and $W_i = \{W_{i1}, W_{i2}, \cdots, W_{im_i}\}$, respectively. Therefore, the UGF for the power output G_i and power demand W_i of all EVSs in the $i-th$ VSS are as follows:

$$\begin{aligned} U_{G_i}(z) &= U_{G_{i1}}(z) \oplus \cdots \oplus U_{G_{i,n_i}}(z) \\ &= \sum_{h=1}^{h_1^i} \alpha_{i,1}^{h_1} z^{g_{i,1}^{h_1}} \oplus \cdots \oplus \sum_{h=1}^{h_{n_i}^i} \alpha_{i,n_i}^{h_{n_i}} z^{g_{i,n_i}^{h_{n_i}}} \\ &= \sum_{a=1}^{A_i} \chi_{i,a} z^{g_{i,a}} \end{aligned} \tag{3}$$

$$\begin{aligned} U_{W_i}(z) &= U_{W_{i1}}(z) \oplus \cdots \oplus U_{W_{i,m_i}}(z) \\ &= \sum_{l=1}^{l_1^i} \beta_{i,1}^{l_1} z^{w_{i,1}^{l_1}} \oplus \cdots \oplus \sum_{l=1}^{l_{m_i}^i} \beta_{i,m_i}^{l_{m_i}} z^{w_{i,m_i}^{l_{m_i}}} \\ &= \sum_{b=1}^{B_i} \delta_{i,b} z^{w_{i,b}} \end{aligned} \tag{4}$$

In equations (3) and (4), A_i represents the total number of power output states for the n_i EVSs in the $i-th$ VSS, and B_i represents the total number of power demand states for the m_i EVSs in the $i-th$ VSS, where $\chi_{i,a} = \Pr\{G_i = g_{i,a}\}$, $\delta_{i,b} = \Pr\{W_i = w_{i,b}\}$.

To further characterize the power output level and power demand level of EVs in the $i-th$ VSS, two indicators, cumulative power s and missing power d are introduced. For all the EVs in the $i-th$ VSS, the power output and power demand are aggregated using the combination operator Ω. The corresponding UGF expression is as follows:

$$\begin{aligned} Q_i(z) &= \Omega(U_{G_i}(z), U_{W_i}(z)) \\ &= \Omega\left(\sum_{a=1}^{A_i} \chi_{i,a} z^{g_{i,a}}, \sum_{b=1}^{B_i} \delta_{i,b} z^{w_{i,b}}\right) \\ &= \sum_{a=1}^{A_i} \sum_{b=1}^{B_i} \chi_{i,a} \delta_{i,b} z^{s=\sum_{a=1}^{A_i} g_{i,a},\, d=\sum_{i=1}^{B_i} w_{i,b}} \\ &= \sum_{v=1}^{V_i} \epsilon_{i,v} z^{s_{i,v}, d_{i,v}} \end{aligned} \tag{5}$$

In the equation (5), V_i represents the total number of combined states. s and d indicate the specific values of accumulated power and missing power for the corresponding the $i-th$ VSS system. Additionally, $\epsilon_v = \Pr\{s = s_{i,v}, d = d_{i,v}\}$.

In practical applications, power loss occurs as power circulates through the system. The magnitude of loss depends on factors such as material properties and equipment operating efficiency. To better illustrate the loss situation, two contrasting scenarios are constructed for system reliability assessment. The first scenario assumes an ideal state with no transmission loss. The second scenario considers transmission loss in actual applications. This quantitatively evaluates the impact of transmission loss on the V2G system.

3.1 Without Considering Transmission Loss

In practical engineering applications, each level of power transmission lines has its own capacity limit. Affected by factors such as environmental disturbances and load variations, the transmission capacity fluctuates and can be treated as a dynamic capacity. The UGF of the transmission capacity C_i^1 for the first level (from the EV cluster to the EVA) is given by equation (6):

$$U_{C_i^1}(z) = \sum_{m=1}^{M_1} \delta_m^1 z^{c_m^1} \tag{6}$$

where $\delta_m^1 = \Pr(C_i^1 = c_m^1)$. In the ideal state, without considering transmission loss, the EVs combine their accumulated power and missing power. Under the constraint of transmission capacity C_i^1, the corresponding UGF is:

$$\begin{aligned} \tilde{Q}_i(z) &= \oplus_*\left(Q_i(z), C_i^1(z)\right) \\ &= \sum_{v=1}^{V_i} \sum_{m=1}^{M_1} \pi_{i,v} \delta_m^1 z^{\min(s_{i,v}, c_m^1), \min(d_{i,v}, c_m^1)} \\ &= \sum_{j=1}^{J_m} \pi_{i,j} z^{\tilde{s}_{i,j}, \tilde{d}_{i,j}} \end{aligned} \tag{7}$$

The combined power is directly transmitted to the EVA through the first-level power transmission lines. The power is then shared for the first time (the surplus power is first used to meet the power demands of EVs in need). The expression is as follows:

$$\begin{aligned}\tilde{Q}_i(z) &= \odot_\varphi\left(\sum_{j=1}^{J_m}\pi_{i,j}z^{\bar{s}_{i,j},\tilde{d}_{i,j}}\right)\\ &= \sum_{j=1}^{J_m}\pi_{i,j}z^{\max(0,\bar{s}_{i,j}-\tilde{d}_{i,j}),\max(0,\tilde{d}_{i,j}-\bar{s}_{i,j})}\\ &= \sum_{j=1}^{J_m}\pi_{i,j}z^{\tilde{s}_{i,j},\tilde{d}_{i,j}}\end{aligned} \tag{8}$$

Based on equation (8), in order to facilitate the reliability assessment of the system, the system's operational states and failure states are separated.

$$\hat{Q}_i(z) = \sum_{f=1}^{F_m}p_{i,f}z^{\bar{s}_{i,f},0} + \sum_{f=1}^{F_n}q_{i,f}z^{0,\bar{d}_{i,f}} \tag{9}$$

where $p_{i,f}$ and $q_{i,f}$ represent the reliability probability and failure probability, respectively. F_m and F_n represent the number of terms corresponding to different states. Specifically, F_m is defined as the number of terms where the surplus power is greater than 0 and the number of terms where both surplus power and missing power are 0. F_n is defined as the number of terms where the missing power is greater than 0.

The reliability of the $i-th$ VSS system can be obtained as follows:

$$R_i = \sum_{f=1}^{F_m}p_{i,f}I(\bar{s}_{i,f}\geq 0) \tag{10}$$

After the first power sharing is completed, the surplus power is transmitted to the EVA and temporarily stored. During peak grid load periods, the stored power is fed back to the grid through the defined second-level power transmission lines (connecting the EVA to the grid). The grid then uses this power to meet the demands of other power-consuming terminals. In this study, it is assumed that each EVA is equipped with a storage unit of a certain capacity.

The power is temporarily stored at the EVA. It is then transmitted to the grid through the second-level power transmission lines. The PMF of C_i^2 can be represented using the UGF as follows:

$$U_{C_i^2}(z) = \sum_{m=1}^{M_2}\delta_m^2 z^{c_m^2} \tag{11}$$

where $\delta_m^2 = \Pr(C_i^2 = c_m^2)$. Next, the combination operator $\oplus_*$ is used for the calculation as shown below:

$$\begin{aligned}V_i(z) &= \oplus_*\left(\overline{Q}_i(z), C_2^i(z)\right)\\ &= \sum_{j=1}^{J_m}\sum_{m=1}^{M_2}\pi_{i,j}\delta_m^2 z^{\min(\bar{s}_{i,j},c_m^2),\min(\bar{d}_{i,j},c_m^2)}\\ &= \sum_{k=1}^{K_i}\rho_{i,k}z^{\hat{s}_{i,k},\hat{d}_{i,k}}\end{aligned} \tag{12}$$

In equation (12), $\hat{s}_{i,k}$ and $\hat{d}_{i,k}$ represent the quantified indicators of surplus power and missing power transmitted from the $i-th$ VSS system to the grid. Subsequently, a new combination operator $\oplus$ is used to aggregate the m VSS systems. The expression for the multi-state aggregation system after power sharing is:

$$\begin{aligned}Q_s(z) &= V_1(z)\widetilde{\oplus}\cdots\widetilde{\oplus}V_m(z)\\ &= \sum_{k_1=1}^{K_1}\rho_{1,k_1}z^{\bar{s}_{1,k_1},\bar{d}_{1,k_1}}\widetilde{\oplus}\cdots\widetilde{\oplus}\sum_{k_m=1}^{K_m}\rho_{m,k_m}z^{\bar{s}_{m,k_m},\bar{d}_{m,k_m}}\\ &= \sum_{k_1=1}^{K_1}\cdots\sum_{k_m=1}^{K_m}\prod_{i}^{m}\rho_{i,k_i}z^{\sum_{i=1}^m\bar{s}_{i,k_i},\sum_{i=1}^m\bar{d}_{i,k_i}}\\ &= \sum_{f=1}^{F_\Omega}P_f z^{S_f,D_f}\end{aligned} \tag{13}$$

In the equation, F_Ω represents the total number of states in the VSG aggregation system. Furthermore, according to the operation rules of equation (8), the surplus power and missing power of the VSG aggregation system are aggregated using the combination operator $\odot_\varphi$.

$$\begin{aligned}\overline{Q}_s(z) &= \odot_\varphi\left(\sum_{f=1}^{F_\Omega}P_f z^{S_f,D_f}\right)\\ &= \sum_{f=1}^{F_\Omega}P_f z^{\max(S_f-D_f,0),\max(D_f-S_f,0)}\\ &= \sum_{f=1}^{F_\Omega}P_f z^{\bar{S}_f,\bar{D}_f}\end{aligned} \tag{14}$$

Without considering transmission loss and transmission capacity constraints, the reliability of the multi-state aggregation system is:

$$R_s = \sum_{f=1}^{F_s}P_f I(\bar{D}_f = 0) \tag{15}$$

where F_s as the number of states that satisfy $\bar{D}_f = 0$, and P_f as the probability of the combined event occurring. When the surplus power is greater than or equal to 0, the VSG aggregation system is considered reliable.

3.2 Consider transmission loss

In practical engineering applications, the accumulated power from EVs can be transmitted through the first-level power transmission lines to the EVA and stored there. During the transmission process, power loss occurs due to the thermal effects of electric currents. Therefore, transmission loss must be considered. The transmission loss rate of the first-level power transmission lines is defined as θ_i^1 $(0 < \theta_i^1 < 1)$. In reality, influenced by load changes, aging of wires, and other environmental factors, the transmission loss rate is also a random variable. In this paper, an exponential decay function is used to represent the transmission loss rate. The mathematical model is expressed as follows:

$$\theta_i^1 = \theta_0 e^{-k_1 t} \tag{16}$$

In the equation, $t \geq 0$ denotes the cumulative operating time of the transmission line since commissioning or last maintenance, with the unit in hours (h). The parameter θ_0 is the baseline transmission loss rate at $t = 0$, selected based on the typical line loss range of 3%–8% in short-distance low-voltage distribution scenarios. The parameter $k_1 \geq 0$ is an empirical decay coefficient reflecting the combined effects of wire aging, environmental interference, and load fluctuations; a larger k_1 indicates faster performance degradation. Similarly, $k_2 \geq 0$ denotes the corresponding decay coefficient for the second-level transmission lines, defined analogously in equation (21). The accumulated power from EVs to the EVA is

$$\min\{s_{iv} \cdot (1 - \theta_i^1), C_i^1\} = \tilde{s}_{iv},$$

and the missing power is

$$\min\{d_{iv} \cdot (1 + \theta_i^1), C_i^1\} = \tilde{d}_{iv}.$$

Considering the transmission capacity constraints, the mathematical model is as follows:

$$\begin{aligned}\tilde{Q}_{i(\text{loss})}(z) &= \otimes_\pi \left(Q_i(z), \theta_i^1, C_i^1(z)\right)\\ &= \sum_{v=1}^{V_m} \sum_{m=1}^{M_1} \mathcal{E}_{i,v} \delta_m^1 z^{\min\{s_{i,v} \cdot (1-\theta_i^1), c_m^1\}, \min\{d_{i,v} \cdot (1+\theta_i^1), c_m^1\}}\\ &= \sum_{j=1}^{J_m} \pi_{i,j} z^{\tilde{s}_{i,j}, \tilde{d}_{i,j}}\end{aligned} \tag{17}$$

Based on the above equation, the specific values of accumulated power and missing power from n_i EVs after passing through the first-level power transmission lines can be accurately calculated. On this basis, power sharing is carried out. The surplus power is fed back to the vehicles in need of power through the first-level power transmission lines.

Furthermore, following the operation rules of equation (8), the surplus power and missing power states of the current $i - th$ VSS are aggregated using the combination operator $\odot_\varphi$. The UGF of this process is expressed as follows:

$$\begin{aligned}\tilde{Q}_{i(\text{loss})}(z) &= \odot_\varphi(\tilde{Q}_{i(\text{loss})}(z))\\ &= \sum_{j=1}^{J_m} \pi_{i,j} z^{\max(0, \bar{s}_{i,j} - \tilde{d}_{i,j}), \max(0, \tilde{d}_{i,j} - \bar{s}_{i,j})}\\ &= \sum_{j=1}^{J_m} \pi_{i,j} z^{\bar{s}_{i,j}, \tilde{d}_{i,j}}\end{aligned} \tag{18}$$

The number of terms in equation (17) is decomposed according to the exponent rules.

$$\hat{Q}_{i(\text{loss})}(z) = \sum_{f=1}^{\hat{F}_m} p_{if} z^{\bar{s}_{i,f}, 0} + \sum_{f=1}^{\hat{F}_n} q_{if} z^{0, \tilde{d}_{i,f}} \tag{19}$$

where $\hat{F}_m$ is defined as the number of terms where the surplus power is greater than 0 and the number of terms where both surplus power and missing power are 0. $\hat{F}_n$ is defined as the number of terms where the missing power is greater than 0. Therefore, the reliability of the $i - th$ VSS system can be obtained as follows:

$$R_{i(\text{loss})} = \sum_{f=1}^{\widetilde{F}_m} p_{if} I(\bar{s}_{i,f} \geq 0) \tag{20}$$

Furthermore, the power is transmitted to the EVA through the second-level transmission lines. Following the calculation paradigm of the first-level transmission lines, the transmission loss rate and transmission capacity of the second-level transmission lines are defined. These parameters are iteratively aggregated using the combination operator $\otimes_\pi$. The UGF of this process is expressed as follows:

$$\begin{aligned} V_{i(\text{loss})}(z) &= \otimes_\pi\left(\hat{Q}_{i(\text{loss})}(z), \theta_i^2, C_i^2(z)\right) \\ &= \otimes_\pi\left(\sum_{v=1}^{\tilde{V}_i} \epsilon_{i,v} z^{\tilde{S}_{i,v},\tilde{d}_{i,v}}, \theta_0 e^{-k_2 t}, \sum_{m=1}^{M_2} \delta_m^2 z^{c_m^2}\right) \\ &= \sum_{v=1}^{\tilde{V}_i}\sum_{m=1}^{M_2} \epsilon_{i,v}\delta_m^2 z^{\min\{\tilde{S}_{i,v}\cdot(1-\theta_i^2),c_m^2\},\min\{\tilde{d}_{i,v}\cdot(1+\theta_i^2),c_m^2\}} \\ &= \sum_{k=1}^{\tilde{K}_i} \rho_{i,k} z^{\tilde{S}_{i,k},\tilde{d}_{i,k}} \end{aligned} \tag{21}$$

Using the combination operator, the m VSS systems are aggregated, and the UGF of the VSG aggregation system is obtained as follows:

$$\begin{aligned} Q_{s(\text{loss})}(z) &= V_{1(\text{loss})}(z)\widetilde{\oplus}\cdots\widetilde{\oplus}V_{m(\text{loss})}(z) \\ &= \sum_{k_1=1}^{\tilde{K}_1} \rho_{1,k_1} z^{\tilde{S}_{1,k_1},\tilde{d}_{1,k_1}}\widetilde{\oplus}\cdots\widetilde{\oplus}\sum_{k_m=1}^{\tilde{K}_m} \rho_{m,k_m} z^{\tilde{S}_{m,k_m},\tilde{d}_{m,k_m}} \\ &= \sum_{k_1=1}^{\tilde{K}_1}\cdots\sum_{k_m=1}^{\tilde{K}_m}\left(\prod_{i=1}^{m}\rho_{i,k_i}\right) z^{\sum_{i=1}^m \tilde{S}_{i,k_i},\sum_{i=1}^m \tilde{d}_{i,k_i}} \\ &= \sum_{f=1}^{\tilde{F}_\Omega} P_f z^{\tilde{S}_f,\tilde{D}_f} \end{aligned} \tag{22}$$

Similarly, according to the operation rules of equation (14), equation (22) is transformed in a consistent manner.

$$\begin{aligned} \bar{Q}_{s(\text{loss})}(z) &= \odot_\varphi\left(\sum_{f=1}^{\tilde{F}_\Omega} P_f z^{S_f,D_f}\right) \\ &= \sum_{f=1}^{\tilde{F}_\Omega} P_f z^{\max(S_f-D_f,0),\max(D_f-S_f,0)} \\ &= \sum_{f=1}^{\tilde{F}_\Omega} P_f z^{\bar{S}_f,\bar{D}_f} \end{aligned} \tag{23}$$

Considering transmission loss and transmission capacity constraints, the reliability of the multi-state aggregation system is:

$$R_{s(\text{loss})} = \sum_{f=1}^{\tilde{F}_s} P_f I(\bar{D}_f = 0) \tag{24}$$

where $\tilde{F}_s$ as the number of states that satisfy $\bar{D}_f = 0$, When the surplus power is greater than or equal to 0, the VSG aggregation system is considered reliable.

4 Case Study Analysis

The previous sections have analyzed the reliability model of the multi-state aggregation system based on V2G technology, considering transmission loss constraints and dynamic variations in transmission capacity. This subsection presents a numerical example for empirical research using EVs as the subject. Two charging station test platforms are constructed, each equipped with four EVs (two in charging mode and two in discharging mode). The specific data are shown in Table 2.

4.1 Without Considering Transmission Loss

The UGF representation of power output and power demand for the EVs in VSS 1 is as follows:

$$U_{G_1}(z) = 0.18z^{52} + 0.12z^{54} + 0.42z^{55} + 0.28z^{57}$$

$$U_{W_1}(z) = 0.08z^{47} + 0.32z^{50} + 0.12z^{52} + 0.48z^{55}$$

Table 2. Output and demand parameters.

	Power Output (kW)	Probability	Power Demand (kW)	Probability
VSS 1	{27, 29} {25, 28}	{0.6, 0.4} {0.3, 0.7}	{30, 25} {25, 22}	{0.6, 0.4} {0.8, 0.2}
VSS 2	{25, 30} {20, 23}	{0.7, 0.3} {0.4, 0.6}	{25, 23} {25, 20}	{0.2, 0.8} {0.5, 0.5}

The result calculated based on equation (5) is as follows:

$$Q_1(z) = 0.0864z^{52,55} + 0.0216z^{52,52} + 0.0576z^{52,50} + 0.0144z^{52,47} + 0.0576z^{54,55} + 0.0144z^{54,52} + 0.0384z^{54,50} + 0.0096z^{54,47} + 0.2016z^{55,55} + 0.0504z^{55,52} + 0.1344z^{55,50} + 0.0336z^{55,47} + 0.1344z^{57,55} + 0.0336z^{57,52} + 0.0896z^{57,50} + 0.0224z^{57,47}$$

The transmission capacity of the first-level power transmission line is denoted as C_1^1. Its power transmission capacity and corresponding probabilities are as follows: when the power transmission capacity is 30 (kW), the probability is 0.4; when the power transmission capacity is 45 (kW), the probability is 0.4; when the power transmission capacity is 60 (kW), the probability is 0.2. The corresponding UGF is expressed as follows:

$$U_{C_1^1}(z) = 0.4z^{30} + 0.4z^{45} + 0.2z^{60}$$

Based on equation (7), the transmission capacity constraint of the first-level power transmission lines is considered as follows:

$$\tilde{Q}_1(z) = 0.4000z^{30,30} + 0.4000z^{45,45} + 0.0029z^{52,47} + 0.0115z^{52,50} + 0.0043z^{52,52} + 0.0173z^{52,55} + 0.0019z^{54,47} + 0.0077z^{54,50} + 0.0029z^{54,52} + 0.0115z^{54,55} + 0.0067z^{55,47} + 0.0269z^{55,50} + 0.0101z^{55,52} + 0.0403z^{55,55} + 0.0045z^{57,47} + 0.0179z^{57,50} + 0.0067z^{57,52} + 0.0269z^{57,55}$$

Based on the combined power output and demand of the EVs in VSS 1, the results after considering the transmission capacity and sharing power are shown below:

$$\tilde{Q}_1(z) = 0.8446z^{0,0} + 0.0115z^{0,1} + 0.0173z^{0,3} + 0.0413z^{2,0} + 0.0101z^{3,0} + 0.0077z^{4,0} + 0.0365z^{5,0} + 0.0198z^{7,0} + 0.0067z^{8,0} + 0.0045z^{10,0}$$

The reliability of VSS 1 is obtained as follows:

$$R_1 = 0.9712$$

Similarly, the UGF representation of power output and demand for the EVs in VSS 2 is as follows:

$$U_{G_2}(z) = 0.28z^{45} + 0.42z^{48} + 0.12z^{50} + 0.18z^{53}$$

$$U_{W_2}(z) = 0.40z^{43} + 0.10z^{45} + 0.40z^{48} + 0.10z^{50}$$

The result calculated based on equation (5) is as follows:

$$Q_2(z) = 0.1120z^{45,43} + 0.0280z^{45,45} + 0.1120z^{45,48} + 0.0280z^{45,50} + 0.1680z^{48,43} + 0.0420z^{48,45} + 0.1680z^{48,48} + 0.0420z^{48,50} + 0.0480z^{50,43} + 0.0120z^{50,45} + 0.0480z^{50,48} + 0.0120z^{50,50} + 0.0720z^{53,43} + 0.0180z^{53,45} + 0.0720z^{53,48} + 0.0180z^{53,50}$$

Similarly, let the power transmission capacity of the first-level power transmission line be denoted as C_1^2. Its power transmission capacity and corresponding probabilities are as follows: when the power transmission capacity is 20 (kW), the probability is 0.3; when the power transmission capacity is 35 (kW), the probability is 0.5; when the power transmission capacity is 50 (kW), the probability is 0.2.

The corresponding UGF is expressed as follows:

$$U_{C_1^2}(z) = 0.3z^{20} + 0.5z^{35} + 0.2z^{50}$$

The UGF after considering the transmission capacity constraint of the first-level power transmission lines is as follows:

$$\tilde{Q}_2(z) = 0.3000z^{20,20} + 0.5000z^{35,35} + 0.0224z^{45,43} + 0.0056z^{45,45} + 0.0224z^{45,48} + 0.0056z^{45,50} + 0.0336z^{48,43} + 0.0084z^{48,45} + 0.0336z^{48,48} + 0.0084z^{48,50} + 0.0240z^{50,43} + 0.0060z^{50,45} + 0.0240z^{50,48} + 0.0060z^{50,50}$$

Table 3. Parameters of the second-level power transmission line.

The second-level power transmission line	Capacity Level (kW)	Probability
VSS 1	35	0.4
	15	0.4
	5	0.2
VSS 2	30	0.3
	20	0.3
	5	0.4

Based on the combined power output and demand of the EVs in VSS 2, the results after considering the transmission capacity and sharing power are shown below:

$$\bar{Q}_2(z) = 0.8452z^{0,0} + 0.0464z^{2,0} + 0.0084z^{3,0} + 0.0396z^{5,0} + 0.0240z^{7,0} + 0.0084z^{0,2} + 0.0224z^{0,3} + 0.0056z^{0,5}$$

The reliability of VSS 2 is:

$$R_2 = 0.9636$$

The UGFs of the second-level power transmission lines are listed in Table 3 as follows:

$$U_{c_1^2}(z) = 0.20z^5 + 0.40z^{15} + 0.40z^{35}$$

$$U_{c_2^2}(z) = 0.40z^5 + 0.30z^{20} + 0.30z^{30}$$

Under the constraints of the second-level transmission capacity, the following mathematical expression is established:

$$V_1(z) = 0.8446z^{0,0} + 0.0115z^{0,1} + 0.0173z^{0,3} + 0.0413z^{2,0} + 0.0101z^{3,0} + 0.0077z^{4,0} + 0.0427z^{5,0} + 0.0158z^{7,0} + 0.0054z^{8,0} + 0.0036z^{10,0}$$

$$V_2(z) = 0.8452z^{0,0} + 0.0084z^{0,2} + 0.0224z^{0,3} + 0.0056z^{0,5} + 0.0464z^{2,0} + 0.0084z^{3,0} + 0.0492z^{5,0} + 0.0144z^{7,0}$$

Under the ideal condition of ignoring transmission loss, the VSS 1 and VSS 2 are aggregated using the combination operator, and the reliability of the multi-state aggregation system is derived as:

$$\begin{aligned} Q_s(z) = {} & 0.713856z^{0,0} + 0.009720z^{0,1} + 0.007095z^{0,2} \\ & + 0.033638z^{0,3} + 0.000258z^{0,4} + 0.004875z^{0,5} \\ & + 0.000452z^{0,6} + 0.000097z^{0,8} + 0.074096z^{2,0} \\ & + 0.000534z^{2,1} + 0.000347z^{2,2} + 0.001728z^{2,3} \\ & + 0.000231z^{2,5} + 0.015631z^{3,0} + 0.000097z^{3,1} \\ & + 0.000085z^{3,2} + 0.000372z^{3,3} + 0.000057z^{3,5} \\ & + 0.008424z^{4,0} + 0.000065z^{4,2} + 0.000172z^{4,3} \\ & + 0.000043z^{4,5} + 0.078460z^{5,0} + 0.000566z^{5,1} \\ & + 0.000359z^{5,2} + 0.001808z^{5,3} + 0.000239z^{5,5} \\ & + 0.000442z^{6,0} + 0.029594z^{7,0} + 0.000166z^{7,1} \\ & + 0.000133z^{7,2} + 0.000603z^{7,3} + 0.000088z^{7,5} \\ & + 0.005420z^{8,0} + 0.000045z^{8,2} + 0.000121z^{8,3} \\ & + 0.000030z^{8,5} + 0.001707z^{9,0} + 0.005672z^{10,0} \\ & + 0.000030z^{10,2} + 0.000081z^{10,3} + 0.000020z^{10,5} \\ & + 0.000156z^{11,0} + 0.001559z^{12,0} + 0.000296z^{13,0} \\ & + 0.000228z^{14,0} + 0.000255z^{15,0} + 0.000052z^{17,0} \end{aligned}$$

Further, the surplus power and missing power of the VSG aggregation system are determined.

$$\begin{aligned} \bar{Q}_s(z) = {} & 0.714814z^{0,0} + 0.011491z^{0,1} + 0.007152z^{0,2} \\ & + 0.033869z^{0,3} + 0.000258z^{0,4} + 0.004875z^{0,5} \\ & + 0.000452z^{0,6} + 0.000097z^{0,8} + 0.000791z^{1,0} \\ & + 0.076154z^{2,0} + 0.016020z^{3,0} + 0.009593z^{4,0} \\ & + 0.078734z^{5,0} + 0.000653z^{6,0} + 0.029675z^{7,0} \\ & + 0.005450z^{8,0} + 0.001707z^{9,0} + 0.005672z^{10,0} \\ & + 0.000156z^{11,0} + 0.001559z^{12,0} + 0.000296z^{13,0} \\ & + 0.000228z^{14,0} + 0.000255z^{15,0} + 0.000052z^{17,0} \end{aligned}$$

The reliability of the multi-state aggregation system is:

$$R_s = 0.941809.$$

4.2 Consider transmission loss

In this subsection, the settings of other parameters remain consistent with the ideal case of ignoring losses. However, the key parameter of transmission loss rate is introduced. In practical application scenarios, if the power transmission lines are short and properly routed, the line transmission loss is typically between 3% and 8%. Assuming that the initial power transmission loss rate for both VSS 1 and VSS 2 is 5% under this model, and considering the effects of aging and environmental factors in the steady-state at $t = 1$, the decay coefficient

$k_1 = 0.005$ is fitted to establish the expression for the transmission loss rate as follows:

$$\theta_1^1 = \theta_2^1 = 0.05e^{-0.005}$$

The transmission losses are not considered to alter the system's calculation logic; therefore, the specific derivation process for this scenario will not be described in detail. Taking into account the constraints of transmission capacity and the impact of transmission loss, the reliability indices for VSS 1 and VSS 2 are determined as follows:

$$R_{1(\text{loss})} = 0.9027$$

$$R_{2(\text{loss})} = 0.8816$$

From the perspective of reliability analysis, the introduction of transmission loss intensifies competition during power sharing and reduces power utilization efficiency to some extent, leading to a noticeable decrease in the reliability of the VSS.

Based on the aforementioned model framework, since the power transmission from the EVA to the grid uses medium- and high-voltage centralized transmission, the current intensity is significantly reduced compared to the first level. Therefore, the expression for the second-level transmission loss rate is defined as follows:

$$\theta_1^2 = \theta_2^2 = 0.03e^{-0.005}$$

After considering both transmission loss and transmission capacity constraints, the reliability of the multi-state aggregation system composed of VSS 1 and VSS 2 is:

$$R_{s(\text{loss})} = 0.802794$$

By taking transmission loss as the only variable and constructing two contrasting scenarios to quantify system reliability, the data results show that the reliability of the multi-state aggregation system decreases from $R_s = 0.941809$ to $R_{s(\text{loss})} = 0.802794$. This demonstrates that transmission loss can significantly reduce system reliability and impact the stability of the power grid.

5 Sensitivity analysis and optimization

5.1 Sensitivity Analysis

To better quantify the impact of transmission loss rate on system reliability, simulations were conducted for VSS 1 and VSS 2 under different transmission loss rates, based on the range of parameter changes. The results are shown in the Figures 2 and 3.

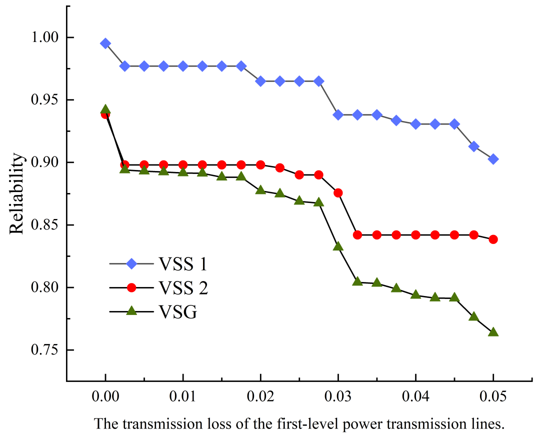

Figure 2. Reliability variation curves of each system with respect to first-level power line loss.

According to Figure 2, as the transmission loss of the first-level power transmission lines increases from 0 to 0.05, the reliability of VSS1, VSS2, and the VSG aggregation system all show a monotonically decreasing trend. This fully verifies that the transmission loss of the first-level power transmission lines is a key factor restricting the reliable operation of the multi-state V2G aggregation system. This conclusion provides a clear direction for improving system reliability in subsequent engineering practice.

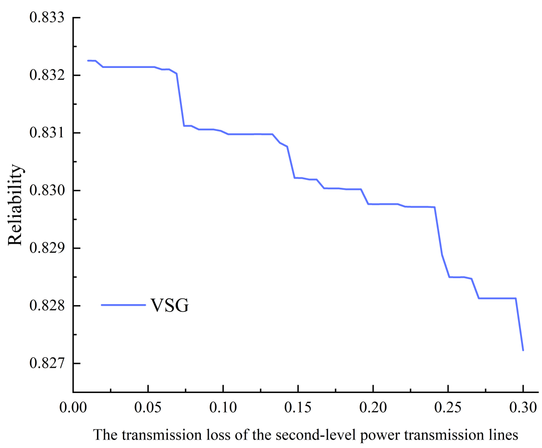

Figure 3. Reliability variation curve of the VSG aggregation system.

According to Figure 3, under the condition that the transmission loss of the first-level power line remains unchanged, as the transmission loss rate of the second-level power line increases from 0 to 0.30, the reliability of the VSG aggregation system shows a monotonically decreasing trend. However, its impact is much weaker than that of the first-level power line.

5.2 Optimization of Power Allocation

In a real engineering scenario, at a large-scale EV charging and swapping station, the number of EVs entering for charging services varies daily. Meanwhile, based on the two-way charging policy, some EVs with surplus power also enter the station to provide excess power. Traditional power allocation methods lack autonomy. When a power gap is detected, the allocation mechanism is triggered, but it does not clearly prioritize charging and discharging EVs. This may lead to congestion during peak times. To address this issue and achieve precise matching and efficient use of power, a scientific power allocation mechanism is needed. This involves collecting detailed vehicle status information using intelligent charging devices and reasonably scheduling power through aggregators. Based on linear programming, this paper sets power supply priorities and proposes an optimization algorithm. The specific algorithm flowchart is shown in Figure 4.

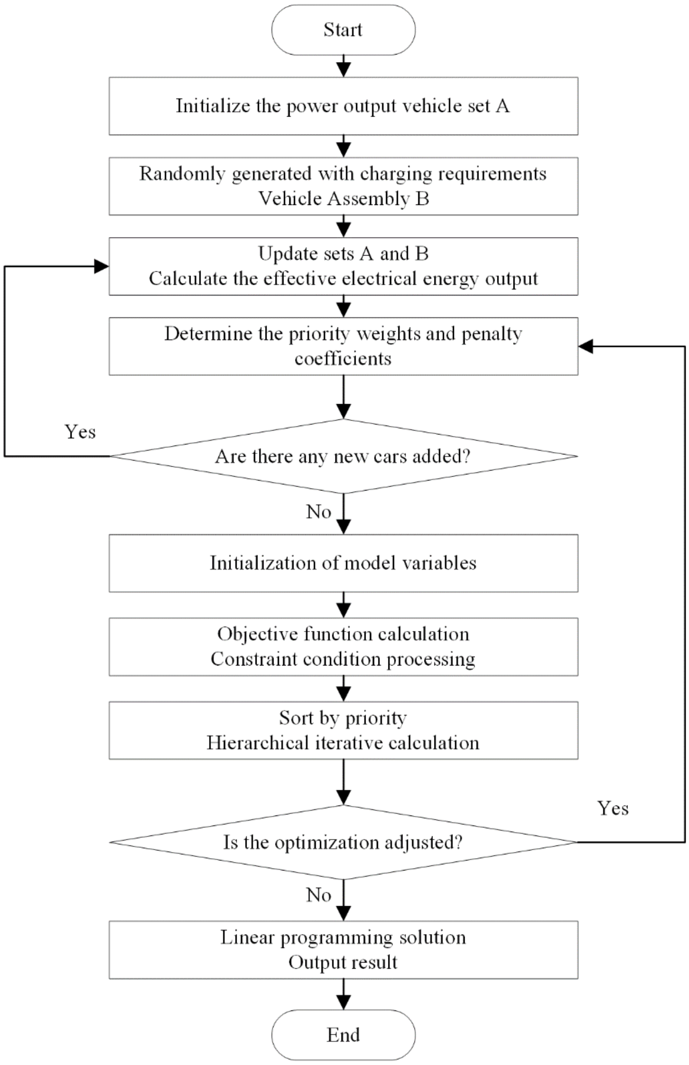

Figure 4. Logical flowchart of the optimization algorithm.

Given that the power output and demand of EVs exhibit discrete multi-state characteristics, to accurately obtain the power output or demand at a specific moment, this paper uses the method of mathematical expectation to calculate. Considering transmission loss, the specific indicators at $t = 1$ are obtained as follows:

$$U_j = \sum_{r=1}^{m} \beta_{jr} g_{jr}^{i} \tag{25}$$

$$G_{\text{total}} = \sum_{j=1}^{n} U_{\text{ef}} = \sum_{j=1}^{n} U_j (1-\theta)^2 \tag{26}$$

where, $\beta_{jr}^{i_r}$ represents the $r-th$ state of the $j-th$ EV under the $i-th$ type of power output, $g_{jr}^{i_r}$ represents the power output in that state, U_{ef} represents the effective power, and G_{total} represents the total effective power output.

This paper defines the range of deep charging for EVs as $(45, 70]$ kW, moderate charging as $(30, 45]$ kW, emergency shallow charging as $(20, 30]$ kW, and balanced maintenance as $(5, 20]$ kW. It also defines the range of deep discharging as $(45, 70]$ kW, moderate discharging as $(30, 45]$ kW, shallow discharging as $(20, 30]$ kW, and trickle charging as $(5, 20]$ kW. Now, assume there are $n = 5$ discharging EVs providing power to the system. The total effective power output after accounting for transmission losses is:

$$G_{\text{total}} = 171.434\,(\text{kW})$$

The charging demand parameters for the EVs on the demand side are shown in Table 4. In the process of constructing the objective function, a weighted deviation method is used to prioritize the power demands, ensuring that high-priority power needs are met first. Based on the magnitude of power demand, the priority order is: deep charging < moderate charging < emergency shallow charging < balanced maintenance. A model that minimizes weighted deviation is constructed. However, to prioritize the needs of more low-power vehicles, some high-power deep charging demands must be sacrificed. A penalty term is introduced to balance the relationship between priority ranking and power optimization.

$$\min Z = \sum_{i=1}^{4} \omega_i (d_i^- + d_i^+) + \alpha \sum_j y_{1j} w_{1j} \tag{28}$$

where α is a penalty coefficient. By adjusting its value, the degree of suppression on deep charging demand can be controlled. Let $\alpha = 1$ and n_1 be the number of vehicles with deep charging demand, and the priority weight is $\omega_1 < \omega_2 < \omega_3 < \omega_4$, $(\omega_1 = 1, \omega_2 = 2, \omega_3 = 3, \omega_4 = 4)$.

Here, d_i^-, d_i^+ represent the negative deviation variable (the part where the actual charging number is less than the target number) and the positive deviation variable (the part where the actual charging number exceeds the target number),

$$\sum_j y_{1j} w_{1j}$$

represents the total power consumption for deep charging, b_i represents the target number of vehicles to be charged for the $i-th$ demand category, y_{ij} represents the $j-th$ vehicle in the $i-th$ demand category, and w_{ij} represents the power demand of the $j-th$ vehicle in the $i-th$ demand category. Based on the principles of goal programming, the following constraints are proposed:

(1) Total Power Constraint (ensuring that the total power for all charging demands does not exceed the total effective power):

$$\sum_{i=1}^{4} \sum_{j=1}^{n_i} y_{ij} w_{ij} \leq G_{\text{total}} \tag{29}$$

(2) Demand Target Constraint (quantifying the difference between the actual number of vehicles charged and the target number):

$$\sum_{j=1}^{n_i} y_{ij} + d_i^- + d_i^+ = b_i \quad (i = 1, 2, 3, 4) \tag{30}$$

(3) Single-Vehicle Allocation Constraint (limiting the charging proportion of each vehicle to no more than 100%):

$$y_{ij} \leq 1 \quad \forall i, j \tag{31}$$

(4) Non-negativity Constraint:

$$y_{ij} \geq 0,\ d_i^- \geq 0,\ d_i^+ \geq 0 \tag{32}$$

Random samples of EVs with charging demands at different stages are generated, as shown in the following Table 4.

Initialize the variables y_{ij}, d_i^-, d_i^+ with initial values of 0. Based on a power allocation strategy prioritizing low power consumption, iterative solutions are obtained. The specific allocation results and final results are shown in Table 5 and Table 6.

In this example, vehicles with deep charging demand were not allocated any power, and the power consumption for deep charging is 0. Therefore:

$$Z = 1(4+0) + 2(1-0) + 3(0+0) + 4(0+0) + 1 \times 0 = 6$$

The vehicles with randomly generated power demands were initially sorted in a certain order: $\{52, 38, 63, 42, 35, 60, 27, 28, 15, 58\}$. If power is allocated to vehicles with power demands in the order of their arrival using traditional charging methods, the system's available power can only meet the charging needs of the first three vehicles $\{52, 38, 63\}$, leaving 18.434 kW units of power remaining. Under this scenario, the power demand satisfaction rate for vehicles is only 30%. The remaining vehicles cannot be charged due to insufficient power, leading to low utilization of the charging station's resources and potentially worsening charging congestion during peak hours. By introducing a dynamic priority-based power allocation mechanism, the system can more rationally distribute the limited power resources. The optimized solution not only covers the charging needs of more vehicles but also increases the satisfaction rate to 50%, reduces user waiting times, and improves the operational efficiency of the charging station.

Through this dynamic power allocation mechanism, the number of vehicles that can be charged is increased, and resource allocation is optimized, even when the total effective power is limited. The intelligent platform automatically identifies and prioritizes low-power charging demands, reducing high-power waste. It implements intelligent delayed scheduling for high-power deep charging demands, allocating their power quotas to more vehicles awaiting charging. This approach selectively sacrifices some high-power deep charging demands to prioritize more low-power vehicles, maximizing service capacity and achieving the optimization logic of "satisfying the majority and deferring the minority." The remaining unallocated power can be temporarily stored by the EVA and flexibly allocated based on the arrival of subsequent vehicles.

Table 4. Distribution of demand for EVs.

Demand Type	Number of Vehicles n_i	Single-Vehicle Generated Charging Demand (kW)	Randomly Generated Charging Demand (kW)
Deep Charging	4	(45,70]	52, 63, 58, 60
Moderate Charging	3	(30,45]	38, 42, 35
Emergency Shallow Charging	2	(20,30]	27, 28
Balanced Maintenance	1	(5,20]	15

Table 5. Allocation result.

Demand Type	Power Demand (kW)	Satisfied Vehicle Number	Remaining Effective Power (kW)	Notes
Balanced Maintenance	15	y_{41}	156.434	–
Emergency Shallow Charging	27, 28	y_{31}, y_{32}	101.434	–
Moderate Charging	35, 38	y_{23}, y_{21}	28.434	Vehicles that cannot be satisfied with y_{22}
Deep Charging	–	–	28.434	Consider the penalty term for vehicles that cannot be satisfied with deep charging demand.

Table 6. Final result.

Demand type	Vehicle ID	Target Number b_i(Vehicle)	Consumed Power (kW)	Total Satisfied Number (Vehicle)	d_i^-	d_i^+
Deep Charging	–	4	0	0	4	0
Moderate Charging	y_{23}, y_{21}	3	73	2	1	0
Emergency Shallow Charging	y_{31}, y_{32}	2	55	2	0	0
Balanced Maintenance	y_{41}	1	15	1	0	0
Total Power Consumption	–	–	143	–	–	–
Remaining Power	–	–	28.434	–	–	–

6 Conclusions

This paper focuses on the multi-state VSG aggregated system under V2G technology.

It uses the UGF method and incorporates the principle of power sharing. Considering factors such as transmission loss and capacity constraints, this study systematically models the multi-state characteristics of EVs, the dynamic changes in transmission capacity, and the two-level transmission losses. It quantifies the multi-state characteristics of each EV and the power loss during transmission. By analyzing the system's reliability in detail, the significant impact of transmission loss rate on system reliability is revealed.

Furthermore, by integrating goal programming algorithms, priority-based power allocation was achieved, effectively increasing the satisfaction rate of EVs with low power demands and reducing resource waste. Case studies validated the practicality of the proposed model in reliability assessment and optimization decision-making, providing a solid theoretical basis for the engineering application of multi-state VSG aggregated systems under V2G technology.

Data Availability Statement

Data will be made available on request.

Funding

This work was supported by the Shanxi Provincial Basic Research Program Youth Project under Grant 202403021212004.

Conflicts of Interest

Peng Su is affiliated with the Shanxi Transportation Technology Research & Development Co., LTD, Taiyuan 030032, China. The authors declare that this affiliation had no influence on the study design, data collection, analysis, interpretation, or the decision to publish, and that no other competing interests exist.

AI Use Statement

The authors declare that no generative AI was used in the preparation of this manuscript.

Ethical Approval and Consent to Participate

Not applicable.

References

[1] Levitin, G. (2011). Reliability of multi-state systems with common bus performance sharing. *IIE Transactions, 43*(7), 518-524. [CrossRef]

[2] Zhao, X., Wu, C., Wang, S., & Wang, X. (2018). Reliability analysis of multi-state k-out-of-n: G system with common bus performance sharing. *Computers & Industrial Engineering, 124*, 359-369. [CrossRef]

[3] Wang, G., Duan, F., & Zhou, Y. (2018). Reliability evaluation of multi-state series systems with performance sharing. *Reliability Engineering & System Safety, 173*, 58-63. [CrossRef]

[4] Qiu, S., & Ming, H. X. (2019). Reliability evaluation of multi-state series-parallel systems with common bus performance sharing considering transmission loss. *Reliability Engineering & System Safety, 189*, 406-415. [CrossRef]

[5] Peng, R. (2019). Optimal component allocation in a multi-state system with hierarchical performance sharing groups. *Journal of the Operational Research Society, 70*(4), 581-587. [CrossRef]

[6] Su, P., Wang, G., & Duan, F. (2020). Reliability evaluation of a k-out-of-n (G)-subsystem based multi-state system with common bus performance sharing. *Reliability Engineering & System Safety, 198*, 106884. [CrossRef]

[7] Jia, H., Liu, D., Li, Y., Ding, Y., Liu, M., & Peng, R. (2020). Reliability evaluation of power systems with multi-state warm standby and multi-state performance sharing mechanism. *Reliability Engineering & System Safety, 204*, 107139. [CrossRef]

[8] Bhatt, V., & Singh, S. B. (2025). Availability analysis of phase mission weighted components system with common bus performance sharing. *Reliability Engineering & System Safety, 260*, 111024. [CrossRef]

[9] Xiao, H., Cao, M., Kou, G., & Yuan, X. (2021). Optimal element allocation and sequencing of multi-state series systems with two levels of performance sharing. *Proceedings of the Institution of Mechanical Engineers, Part O: Journal of Risk and Reliability, 235*(2), 282-292. [CrossRef]

[10] Cheng, C., Yang, J., & Li, L. (2021). Reliability evaluation of a k-out-of-n (G)-subsystem based multi-state phased mission system with common bus performance sharing subjected to common cause failures. *Reliability Engineering & System Safety, 216*, 108003. [CrossRef]

[11] Su, P., Wang, G., & Duan, F. (2021). Reliability analysis for k-out-of-(n+ 1): G star configuration multi-state systems with performance sharing. *Computers & Industrial Engineering, 152*, 106991. [CrossRef]

[12] Yi, K., Xiao, H., Kou, G., & Peng, R. (2019). Trade-off between maintenance and protection for multi-state performance sharing systems with transmission loss. *Computers & Industrial Engineering, 136*, 305-315. [CrossRef]

[13] Azhdari, A., & Ardakan, M. A. (2022). Reliability optimization of multi-state networks in a star configuration with bi-level performance sharing mechanism and transmission losses. *Reliability Engineering & System Safety, 226*, 108556. [CrossRef]

[14] Wu, C., Pan, R., & Zhao, X. (2022). Reliability assessment of multi-state performance sharing systems with transmission loss and random shocks. *IISE Transactions, 54*(11), 1060-1071. [CrossRef]

[15] Wu, C., Zhao, X., Wang, S., & Song, Y. (2025). Reliability analysis of weighted k-out-of-n: G performance sharing systems with multiple transmission loss levels. *Reliability Engineering & System Safety, 257*, 110859. [CrossRef]

[16] Gu, L., Wang, G., & Zhou, Y. (2025). Reliability analysis and optimization of multi-state tree-structured systems with performance sharing mechanism. *Reliability Engineering & System Safety, 260*, 110990. [CrossRef]

[17] Liu, J., Zhuge, C., Tang, J. H. C. G., Meng, M., & Zhang, J. (2022). A spatial agent-based joint model of electric vehicle and vehicle-to-grid adoption: A case of Beijing. *Applied Energy, 310*, 118581. [CrossRef]

[18] Ma, S. C., Fan, Y., Yao, X., Fang, H., & Xu, C. (2025). Cost and environmental impacts assessment of electric vehicles and power systems synergy: The role of vehicle-to-grid technology. *Environmental Impact Assessment Review, 114*, 107899. [CrossRef]

[19] Peng, C. (2019). *Charge park vehicle-to-grid service: Modeling, control, and optimization* (Doctoral dissertation, University of Nebraska–Lincoln). ETD Collection for University of Nebraska–Lincoln. Digital Commons UNL. https://digitalcommons.unl.edu/dissertations/AAI13902940

[20] Lee, W., Woo, J., Kim, Y. G., & Koo, Y. (2024). Vehicle-to-grid as a competitive alternative to energy storage in a renewable-dominant power system: An integrated approach considering both electric vehicle drivers' willingness and effectiveness. *Energy, 310*, 133194. [CrossRef]

[21] Sagaria, S., Van Der Kam, M., & Boström, T. (2024). The influence of socio-technical variables on vehicle-to-grid technology. *Energy, 305*, 132299. [CrossRef]

[22] Liu, F., Wei, Z., Lin, Y., Huang, X., Li, Y., Huang, Y., & Lim, M. K. (2025). Vehicle-To-Grid Technology Acceptance for Electric Vehicle Users: A Systematic

Literature Review and Future Research Agenda. *International Journal of Consumer Studies*, *49*(3), e70065. [CrossRef]

[23] Su, P., Yang, X., Peng, R., Hu, L., & Li, T. (2026). Reliability analysis of multi-state aggregation power grid systems under the Vehicle-to-Grid mode. *Reliability Engineering & System Safety*, 112446. [CrossRef]

[24] Comi, A., & Elnour, E. (2024). Challenges for implementing vehicle-to-grid services in parking lots: A state of the art. *Energies*, *17*(24), 6240. [CrossRef]

[25] Du, Y., Zhang, J., Chen, Y., Liu, Z., Zhang, H., Ji, H., ... & Yan, J. (2025). Impact of electric vehicles on post-disaster power supply restoration of urban distribution systems. *Applied Energy*, *383*, 125302. [CrossRef]

[26] Kouzelis, A., Linders, K., Bandyopadhyay, S., & Mouli, G. R. C. (2025). Analysis of vehicle-integrated photovoltaics and vehicle-to-grid on electric vehicle battery life. *Journal of Power Sources*, *631*, 236117. [CrossRef]

[27] Li, T., Tao, S., He, K., Lu, M., Xie, B., Yang, B., & Sun, Y. (2021). V2G multi-objective dispatching optimization strategy based on user behavior model. *Frontiers in Energy Research*, *9*, 739527. [CrossRef]

[28] Prencipe, L. P., Van Essen, J. T., Caggiani, L., Ottomanelli, M., & de Almeida Correia, G. H. (2022). A mathematical programming model for optimal fleet management of electric car-sharing systems with vehicle-to-grid operations. *Journal of Cleaner Production*, *368*, 133147. [CrossRef]

[29] Shaheen, H. I., Rashed, G. I., Yang, B., & Yang, J. (2024). Optimal electric vehicle charging and discharging scheduling using metaheuristic algorithms: V2G approach for cost reduction and grid support. *Journal of Energy Storage*, *90*, 111816. [CrossRef]

[30] Liu, K., Liu, Y., Si, G., Lu, X., & Xie, Y. (2025). Punctual V2G scheduling circle: Evaluate and enhance transfer V2G capability through adaptive redistribution. *Applied Energy*, *383*, 125290. [CrossRef]

[31] Zhang, H., Hu, Z., Xu, Z., & Song, Y. (2016). Evaluation of achievable vehicle-to-grid capacity using aggregate PEV model. *IEEE Transactions on Power Systems*, *32*(1), 784-794. [CrossRef]

Xu Yang received his B.S. degree in Industrial Engineering from North University of China in 2023 and is currently pursuing his M.S. degree there. His research interests focus on reliability modeling and performance evaluation of multi-state complex systems. (Email: xuy_0415@163.com)

Peng Su received the Ph.D. degree in mathematics from the School of Mathematics, Southeast University, Nanjing, China, in 2020. He is currently an Associate Professor with the School of Economics and Management, North University of China. His research interests include stochastic modeling, fuzzy reliability modeling, V2G technology research. (Email: supeng@nuc.edu.cn)

Yuzhe Dong is a postgraduate student at the School of Vehicle and Transportation Engineering at Taiyuan University of Science and Technology in China. His research interests include intelligent transportation systems, traffic flow modeling, and transportation system optimization. (Email: DongYZ9829@163.com)